One-, Two- and Three Dimensional Structures in Thermotropic Liquid Crystals

S. Diele [a] , S. Grande [b] , J. Kain [a] , G. Pelzl [a] & W. Weissflog [a]

[a] Institut für Physikalische Chemie, Martin-Luther-Universität Halle-Wittenberg, Mühlpforte 1, D-06108, Halle, Germany

[b] Fakultät für Physik und Geowissenschaften, Universität Leipzig, Linnestr. 5, D-04103, Leipzig, Germany

Version of record first published: 24 Sep 2006

PLEASE SCROLL DOWN FOR ARTICLE

One-, Two- and Three Dimensional Structures in Thermotropic Liquid Crystals[*]

S. DIELE[a†], S. GRANDE[b], J. KAIN[a], G. PELZL[a] and W. WEISSFLOG[a]

[a]*Institut für Physikalische Chemie, Martin-Luther-Universität Halle-Wittenberg, Mühlpforte 1, D-06108 Halle, Germany and* [b]*Fakultät für Physik und Geowissenschaften, Universität Leipzig, Linnestr. 5, D-04103 Leipzig, Germany*

In two homologous series of bi-swallow tailed compounds transitions between lamellar (SmC), columnar (Col$_{rect}$) and three-dimensional (T) phases have been studied by X-ray and NMR-methods. The NMR studies yield the conformation of the molecule, whereas the X-ray studies of monodomains provide information about the lattice type and the symmetry.

Keywords: polycatenar compounds; columnar phase; tetragonal phase; X-ray studies; NMR studies

INTRODUCTION

The field of thermotropic liquid crystalline phases has been dominated over a long time by rod-like molecules, which form mainly nematic or smectic phases. The smectic liquid crystalline phases may be considered as a one-dimensional array of liquid layers. The introduction of a special interaction by the substitution of special groups, e.g. polar groups[1–4] or chemical incompatible groups[5–12] leads to a frustration in the packing of the rod-like molecules and to an additional periodicity, perpendicular or inclined to the layer normal. In this way a two-dimensional structure results.

In lyotropic systems which were formed by amphiphilic molecules, like detergents or lipids, such structures have been well-known over years. Already in 1957 LUZZATI. MUSTACCHI and SKOULIOS[13] reported about one- and two-dimensional structures observed in soap-water systems. In 1961[14] again SKOULIOS and LUZZATTI published results of X-ray investigations at pure

---

* Dedicated to Professor Skoulios on the occasion of his 65thbirthday
† Author of correspondence.

(water-free) sodium soaps, which not only proved the existence of one-dimensional lamellar and two-dimensional structures at heating, but also – in the case of Natrium laurate – the existence of a three-dimensional orthorhombic centred cell. The orthorhombic cell was described to be formed by disc-like plates of the former lamellar structure. After this pioneering work numerous investigations in lyotropic systems have been performed, which led to a detailed knowledge of the structure of these phases. Besides the two-dimensional hexagonal phase and the three-dimensional cubic phases, with micellar and bi-continuous structures, orthorhombic, tetragonal and rhombohedral phases are known. (see[15] and references found therein).

The important role of the hydrogen bonds for the structure formation, as found in lyotropic systems between the hydrophilic head groups and the water molecules, can be observed in thermotropic systems, too. The amhiphilic molecules tend to segregate their amphiphatic moieties in distinct regions. The ratio between the head groups and the aliphatic tails and -connected with this- the curvature of the interface between both of them determine the kind of structure. (see[16,17] and references found therein).

Polycatenar mesogens consist of a rod-like rigid core and of one or two half-disc shaped moieties at the end because of the terminal branches[18–27]. With respect to a dense packing they can be regarded as frustrated systems because of the different cross-sections of the core and the branches. Depending on the length and structure of the core and on the number, position and length of the terminal chains polycatenar liquid crystals exhibit nematic, lamellar (SmC) and columnar phases (Col$_{hex}$, Col$_{obl}$, Col$_{rect}$)[19,20]. There are also some tetracatenar compounds (bi-forked compounds) which show transitions between lamellar and columnar phases and between columnar and a three-dimensional phase[20–25]. The transition from the lamellar into the columnar phase was explained by the breaking of the smectic layers because of the unfavourable packing resulting from the segregation of aromatic cores on one side and the bulky disordered aliphatic tails on the other side [25,26]. The two-dimensional cell of the columnar phase is obviously built up by layer fragments, the thickness of which is nearly equal to the layer spacing in the SmC phase. In some respect this process is quite similar to that of the ribbon phase of thermotropic alkali soaps[14]and of the terminal polar compounds[1]. The tendency of the separation into aromatic core regions (hydrophilic part) and aliphatic regions (hydrophobic part) and the balance between both of them is used for an interpretation of the structure on the base of a bi-continuous minimal surface in analogy to the discussion in lyotropic systems[28].

In principle, the so-called double-swallow-tailed compounds can be regarded as a special variant of the tetracatenar compounds in which the terminal branches
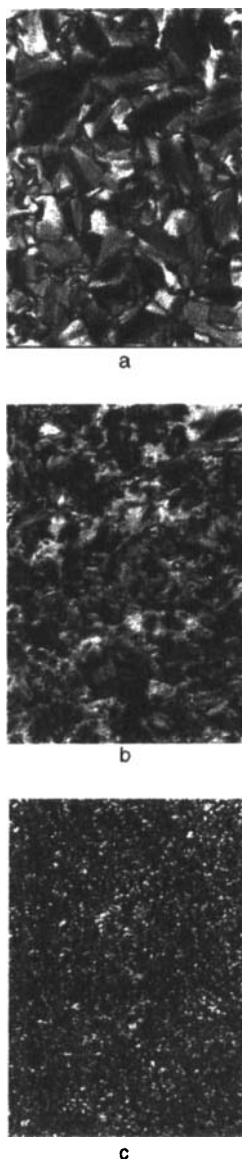
FIGURE 1 Textures of compound **B6–13** in the a) SmC phase, b) Col phase and c) T phase (See Color Plate I at the back of this issue)

are not directly attached to the terminal rings but via a linkage group. Therefore it is not surprising that the phase behaviour shows similarities to the bi-forked

compounds, e.g. a transition between lamellar, columnar and three dimensional rhombohedral phases could be detected[29–34]. Using new experimental techniques on these compounds beside the cubic phases additional three-dimensional structures have been observed which shall be presented in the following.

EXPERIMENTAL

The most essential progress in our work could be achieved by using a simple sample preparation to orient the samples. A small drop of the sample was heated on a cleaned glass plate up to the isotropic state and cooled down slowly to the temperature of investigation. In this way the samples of most compounds could be aligned by the surface interaction.

The X-ray beam is incident parallel to the glass plate and the scattered intensity was recorded by a two-dimensional detector (HI-STAR, Siemens AG, Germany). The patterns proved the existence of a monodomain or of an aligned sample with rotational disorder around the normal of the glass plate. This method led to results which gave rise to a re-interpretation of the structures, only based on the studies of non-oriented samples.

Beside the standard methods like Guinier methods for structure investigations polarizing microscopy and DSC for the phase characterization and investigation of phase transitions have been used.

The NMR measurements were performed using a Bruker MSL 500 spectrometer at a field of 11.7 T. The temperature of the 5 mm sample tubes was regulated by a Bruker BST-100 temperature controller. Most lines are resolved in the proton decoupled ^{13}C spectra at 125 MHz. The amplitude of the decoupling field in the liquid crystalline phases was as low as possible (0,6–0,8 mT) in order to avoid a heating of the sample. Simple pulse excitations and cross-polarisation experiments with continuous – or pulsed – decoupling are used. In the former case an offset of the proton frequency (0.5 – 3 kHz against ^{1}H methylene resonance) influences the efficiency of the decoupling and helps in the identification of the lines.

INVESTIGATED SUBSTANCES

The Tables I and II summarize the transition temperatures and -in brackets- the transition enthalpies of the substances under discussion.

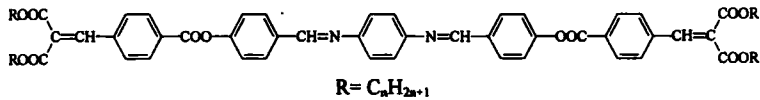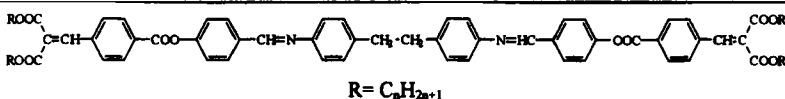TABLE I Transition temperatures and enthalpies (kJmol^{-1}) of series A

R= C_nH_{2n+1}

Compound	n					Polymorphism					
A5–10	10	Cr	99 [52.8]	SmC	149 [1.71]	N	198 [0.26]	I			
A5–11	11	Cr	95 [60.5]	SmC	151 [2.04]	N	193 [0.26]	I			
A5–12	12	Cr	96 [94.5]	T	106 [0.49]	SmC	147 [1.92]	N	171 [0.23]	I	
A5–13	13	Cr	96 [107.6]	T	128 [0.97]	SmC	144 [2.01]	N	150 [0.31]	I	
A5–14	14	Cr	101 [119.0]	T	136 [1.24]	SmC	142 [2.42]	I			
A5–16	16	Cr	103 [128.0]	T	134 [3.93]	I					

TABLE II Transition temperatures and enthalpies (kJmol^{-1}) of series B

R= C_nH_{2n+1}

Compound	n					Polymorphism					
B6–12	12	Cr	95 [54.4]	SmC$_{re}$	117 [0.20]	Col$_{rect}$	154 [0.40]	SmC	187 [2.43]	N	209 [0.30]	I
B6–13	13	Cr	102 [101.9]	T	162 [0.10]	Col$_{rect}$	165 [1.97]	SmC	184 [2.58]	I		
B6–16	16	Cr	104 [101.8]	T	178 [5.41]	I						

The phases have been characterized first by their textures observed in the polarizing microscope. The Figure 1 displays specific textures.

The SmC phase appears as a broken fan-shaped texture or as a Schlieren texture, whereas the low temperature phase of the series A and B is observed with a nonspecific texture, which strongly depends on the sample preparation.
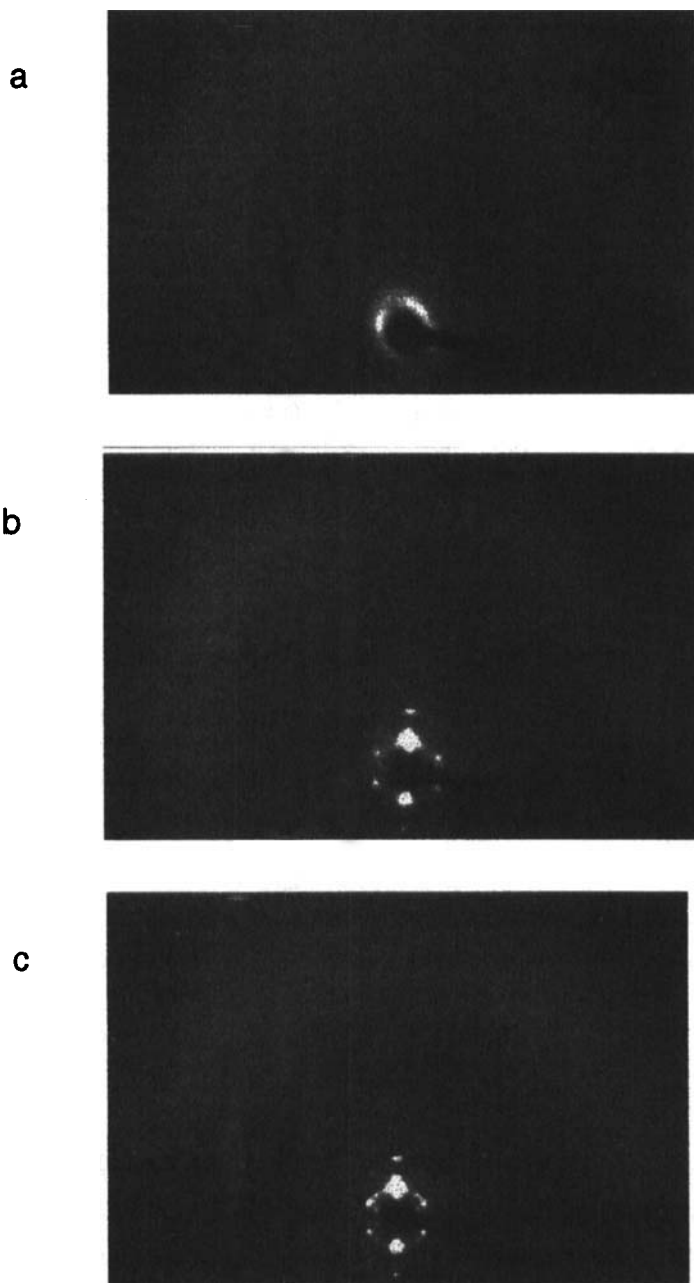
S. DIELE *et al.*

FIGURE 2 X-ray patterns of an oriented sample of compound A5–13 in the a) N phase b) SmC phase and c) T phase (See Color Plate II at the back of this issue)

X-RAY STUDIES

Figure 2 displays the changes of the patterns of compound **A5–13** with decreasing temperature.

In the N phase the dumb-bell like scattering in the small-angle region proves the existence of cybotactic groups. The spot-like reflections on the meridian of the pattern of the SmC phase indicate a re-orientation of sample. The smectic layer normal is parallel to the normal of the glass plate. In the N phase as well as in the SmC phase the outer diffuse scattering appears as a closed ring which is superimposed by a diffuse maximum, positioned only at one side of the meridian and forming an angle $\chi = 30°$ with the meridian. This diffuse maximum can be attributed to the aromatic moiety of the molecules, whereas the closed diffuse ring is caused by the disordered aliphatic chains.
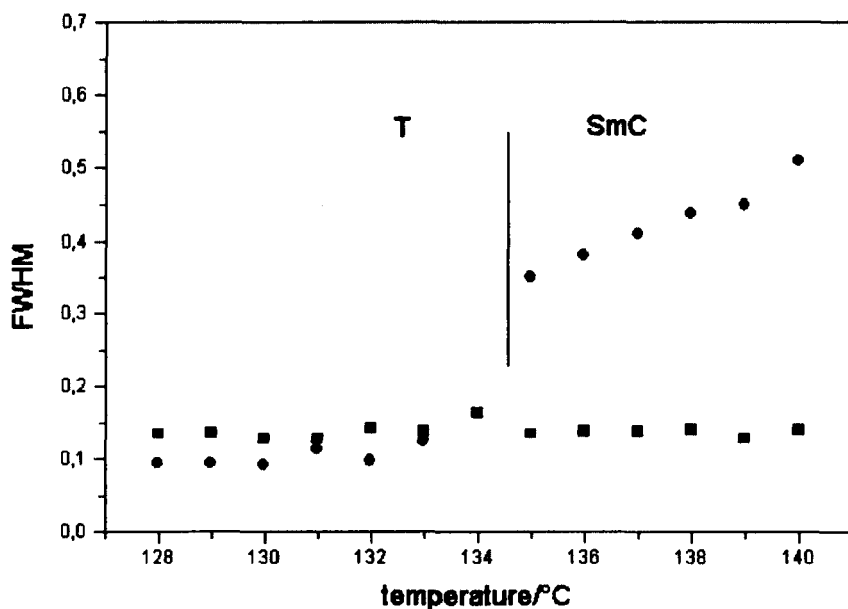
FIGURE 3 Full width at half maximum (FWHM) of the out of meridian reflections (filled circles) in comparison to that of the second order of the layer reflection (sqares) as the function of the temperature (See Color Plate III at the back of this issue)

Cooling down the sample, additional scattering maxima appear within the SmC phase in the small angle region of the pattern outside the meridian. They indicate the appearance of a periodicity perpendicular to the layer normal. But

the measurements of the full width at half maximum (FWHM) prove the diffuse character of the scattering. Figure 3 shows the temperature dependence of the FWHM of the scattering (circles) in comparison to that of the second order of the layer reflection (squares). That means that the periodicity remains limited to a short range order in the SmC phase and does not lead to a phase transition into a two-dimensional phase. At the transition into the low-temperature phase the additional diffuse scattering condenses to Bragg-spots with an instrumentally limited line width. But simultaneously a lot of Bragg-spots can be observed in the small angle region. (see Figure 2c). Furthermore, the diffuse outer scattering is positioned symmetrically to the meridian, now. This pattern is typical for all low temperature phases listed in Tables I and II.
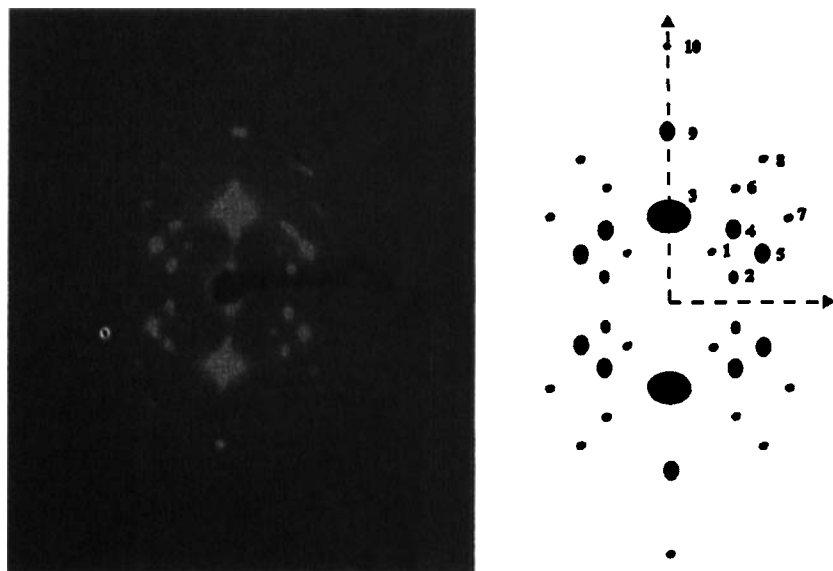
FIGURE 4 Small angle region of Figure 2c and a sketch of the observed reflections (See Color Plate IV at the back of this issue)

In the compound **B6–13** a columnar phase appears between the SmC phase and the low temperature phase. In this phase the period perpendicular to the layer normal accepts a quasi long range order. It could be proved because the out of meridian reflections exhibit now the instrumentally limited line width. It should be noted, that the transition into the intermediate columnar phase was also recognized by microscopic investigations (see Figure 1b), but could not be detected by calorimetry. The pattern of the low temperature phase (the enlarged small angle

region is shown and sketched in Figure 4) displays a lot of Bragg-spots positioned on lines parallel to the c^* axis which cannot be attributed to a two-dimensional lattice. Therefore a three-dimensional cell is assumed and the pattern is evaluated under the following assumptions:

-   based on the rotational disorder around the normal (equal to the c^* axis of the reciprocal space) planes with different h and k indices can simultaneously be observed.
-   only 001 reflections with l = 4n are allowed
-   the lattice axes form an angle of 90 degrees.
-   further extinction rules could not be observed.

The serial extinction for 001 reflections with l ≠ 4n along the c^* axis demands a 4-fould screw axis parallel to the c axis. A 4-fould axis can be found only in a tetragonal system or in the cubic system, the latter one can be excluded in this case. (Therefore the third assumption is a consequence of the second one.) In Table III the measured and calculated Bragg-angles of the tetragonal phase of the series A and B are listed. The agreement between the measured and calculated values is good, since the experimental error, especially at the small angles (for the weak reflections 1 and 2), is higher.

NMR STUDIES

To obtain more detailed information about the molecular conformation in the liquid crystalline state NMR measurements have been performed.

The starting point for the interpretation of spectra in the isotropic and liquid crystalline phases is the assignment of the peaks. The numeration of the positions for **B6–13** is given in Figure 5.
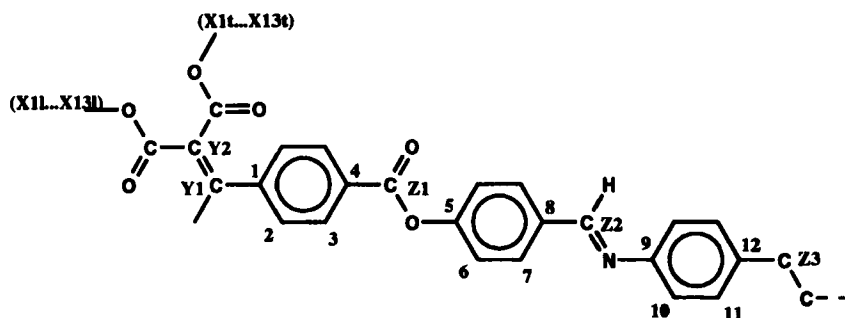

FIGURE 5 Molecular structure and labelling of the atoms

TABLE III Observed and calculated Bragg angles in the T phase

	A5–13		5A-14		5A-16		B6–13		B6–16	
ection	θ_{exp} in °	θ_{cal} in °	θ_{exp} in °	θ_{cal} in °	θ_{exp} in °	θ_{cal} in °	θ_{exp} in °	θ_{cal} in °	θ_{exp} in °	θ_{cal} in °
	0.89	0.79	0.88	0.80	0.92	0.82	0.87	0.78	0.78	0.75
	0.94	0.85	0.93	0.85	0.96	0.88	0.85	0.84	0.84	0.81
	1.14	1.12	1.13	1.13	1.13	1.14	1.08	1.09	1.03	1.03
	1.22	1.16	1.22	1.17	1.22	1.19	1.16	1.14	1.11	1.09
	1.26	–	1.27	–	1.31	–	1.25	–	1.21	–
	–	–	1.69	1.63	–	–	–	–	–	–
	1.73	1.69	1.74	1.70	1.74	1.74	1.65	1.66	1.60	1.60
	2.00	2.03	2.04	2.04	2.05	2.08	1.99	1.99	1.87	1.89
	2.25	–	2.27	–	2.29	–	2.19	–	2.06	–
	3.38	3.37	3.32	3.39	–	–	–	–	–	–

The assignment of the lines in the isotropic spectrum as shown in Figure 6 is based on the increment system and the comparison with similar substituted aromatic rings.
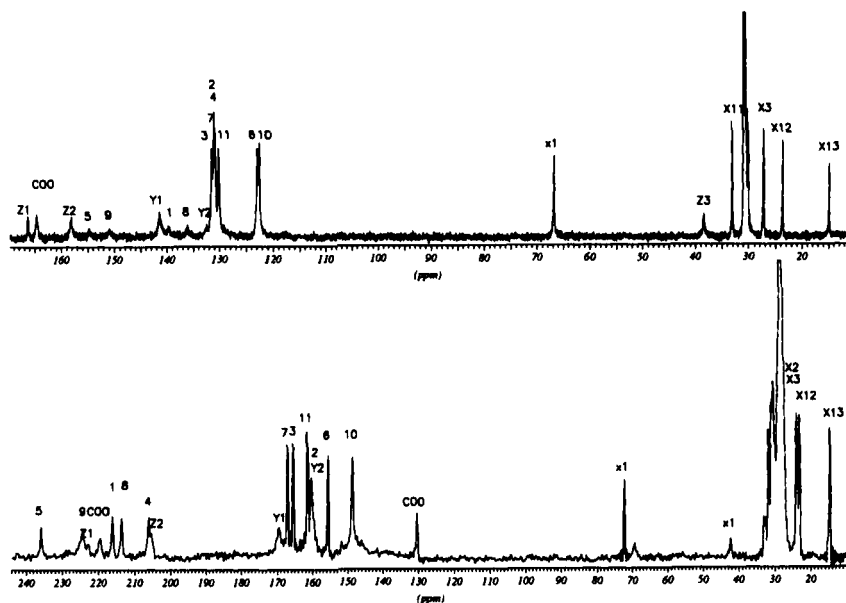

FIGURE 6 ^{13}C spectra of **B6–13** in the isotropic (above) and smectic (below) phase with the assignment of the lines. The NOE increases the intensity of the protonated lines in the isotropic spectrum. The spectrum of the smectic phase was measured with CP and pulsed decoupling

The lines from carbon atoms belonging to symmetrically equivalent positions of the molecule always coalesce in the spectra at all temperatures. The lines of the para-positions are broadened in the isotropic spectra. All measurements are carried out by lowering the temperatures. The transition to the liquid crystalline phases occurs within 2 K for both substances. A few lines in the SmC phase (see Figure 6) are broadened due to the C-N dipole interaction (C9 and Z2) or incomplete decoupling. In our experiments the director orients parallel to the strong external field and the layer normals are tilted. The spectra therefore contain no information about the tilt angle in the SmC phase.

In **A5–13** a strong temperature variation of the shifts below the clearing temperature and a jump at the transition to the SmC phase is observed. **B6–13** also forms a nematic phase after repeated measurements caused by a partial decomposition. The observed temperature dependence of the ^{13}C chemical shift is related to the order parameter S by a simple equation

$$\delta^i{}_{obs}(T) = \delta^i{}_{iso} + S\delta^i_{\zeta\zeta}$$

Within this work the small contributions from the biaxality order parameter D is neglected. The $\delta^i_{\zeta\zeta}$ are the components of the shift tensor in the molecular system ξ, η, ζ with ζ as molecular long axis. ζ deviates only by a few degrees from the para-axis of the aromatic rings and the angles of the equivalent rings on the right and left side must agree.

The observed anisotropy is the result of order and geometry of the considered segment. The exact main frame tensor components for the different positions are not known. Our further conclusions are therefore based on the comparison with liquid crystalline reference compounds without knowing exactly all three components of the shift tensors. We calculate the $\delta^i_{\zeta\zeta}$ in the aromatic region from the ratios of the anisotropic shifts. The appointment of one position ($\delta^{C5}_{\zeta\zeta} = 94$ ppm in **A5–13** and **B6–13**), derived from the results of similar molecules, then defines the long axis values of all carbon shifts and allows the calculation of S for the central part. This procedure already includes our approximate model that the molecular long axis has a similar orientation as in classic two ring molecules. The obtained S values for the two samples are shown in Figure 7. We recognize the typical temperature dependence of the order parameter for a nematic phase (followed by a smectic one for the **A5–13**) and the strong jump at the transition to the SmC phase. The order parameter in the SmC phase is higher than for most classic two ring compounds. In **B6–13** the order in SmC starts with high values in agreement with **A5–13**. The nematic phase of the aged samples behaves similarly to **A5–13**. The correctness of the above derived ^{13}C tensor components is supported by the evaluation of the ^{1}H dipolar splitting, that delivers the same S values for a typical H-H distance of 0.248 pm.

After fixing $\delta^{C5}_{\zeta\zeta}$ also most of the other tensor components $\delta^i_{\zeta\zeta}$ of the central part agree with the corresponding values of two ring molecules. This justifies the conclusion, that the geometry of the central part of the long molecules with respect to the direction of the molecular long axis is indeed similar. The resolution of two different signals from the ester groups and the neighbouring methylene groups in the swallow tails explains the conformation and geometry of the two chains. This is best demonstrated by a comparison of the tensor components $\delta^i_{\zeta\zeta}$ in Table IV. We obtained similar results in both substances. COO(I) has a $\delta^i_{\zeta\zeta}$ similar to the linkage group of the reference compounds as expected due to the equivalent geometry. The anisotropy of the other group, COO(t), even has an opposite sign. This can only be explained, if we assume that the plane of the unit orients perpendicular to the plane formed by the neighbouring -C=C-C(OO) group. The same argument applies to the α-methylene group. Usually the shift anisotropy of the CH$_2$-groups in the chains are negative (shown for reference in Table IV). The O-CH$_2$(I) bond orients more parallel to the long axis than in typical alkoxy-chains. This increases the anisotropy, whereas the nearly perpendicu-
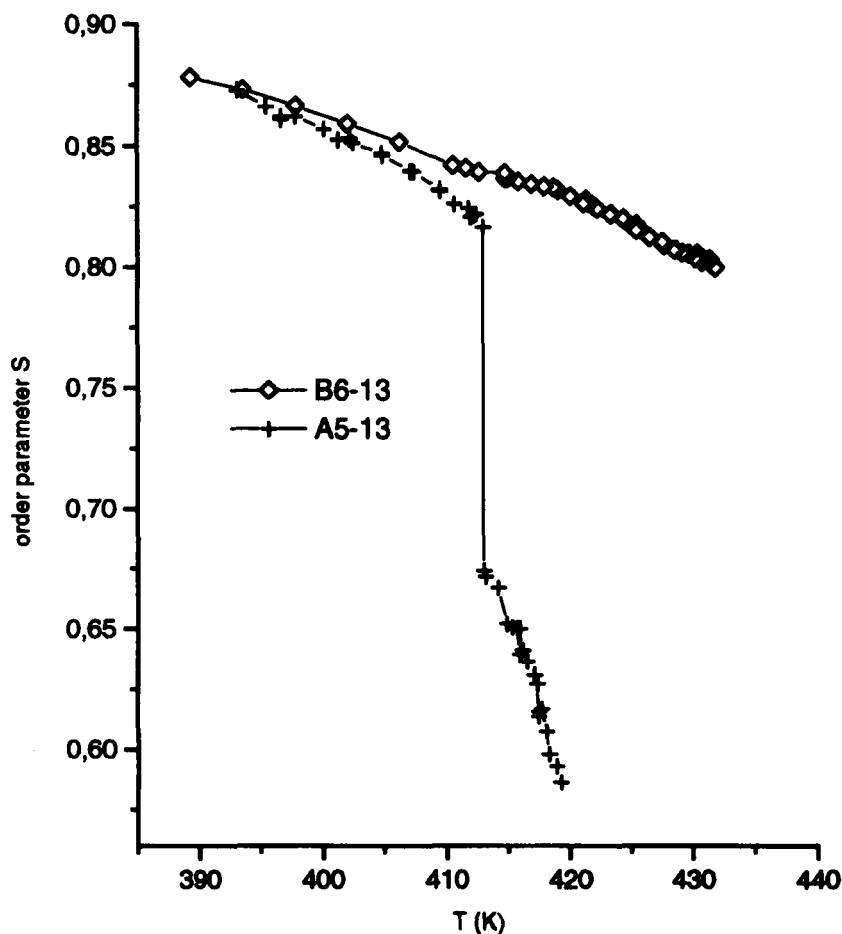
FIGURE 7 Order parameter S of the central part of the molecules **B6–13** and **A5–14**. They are evalu-ated from the anisotropic shifts using $\delta^{C5}_{\zeta\zeta} = 94$ ppm

lar orientation of O-CH$_2$(t) bond inverts the sign of the shift anisotropy. For the following segments the expected even-odd effect along one chain and the differ-ence of the tensor components between the two chains disappears. The two chains can not be distinguished after the third segment. The comparatively low value of $\delta^{x3}_{\zeta\zeta}$ and of the following segments supports the presumption that the averaged chain axes are parallel to each other after the γ-methylene group and tilted with respect to the central molecular axis. If we compare the observed ani-sotropies with the reference values in Table IV a tilt angle of roughly 40° between the two axis can be estimated.

TABLE IV Tensor components $\delta^i_{\zeta\zeta}$ for the chain segments. (I indicates the chain directed parallel to the molecular long axis and t the second chain. The last column gives the values of a common rod-like compound in the liquid-crystalline state)

Pos.	I (ppm)	t (ppm)	Refer (ppm)
COO	60.8	−38.5	61.5
x1	−28.9	5.8	−9.6
x2	−7.5	−3.5	−10.0
x3	−4.2	0.2	−9.0
xm	−3.0		−8.0
x10	−2.6		
x11	−2.2		
x12	−1.1		
x13	−0.75		

Results in the low temperature phase

Both materials transform to a low temperature phase below the SmC phase. The transition changes the NMR spectra dramatically. Instead of sharp lines we only observe broad bands in the ^{13}C spectra (see Figure 8). The opposite occurs in the proton spectra, the line width of the strong central line of the aliphatic protons decreases by a factor of 2.

A typical feature of classic columnar phases is the orientation of the column axis (director) perpendicular to the magnetic field in the NMR experiments. This suggests a continuous distribution of azimuth angles of the long molecular axes inside the column, since then the magnetic energy is minimized. The perpendicular column axis reduces all NMR anisotropies by −1/2. Their components along the director deviate from the values along the long molecular axis in the smectic phase. The exact value depends on the arrangement and the dynamics of the molecules in the columns. For a static distribution and a tilt angle β between the molecular and columnar axes we obtain a cylindrical powder spectrum in the NMR with sharp singularities at shift values.

$$\delta_{\zeta\zeta cyl} = \delta_{\zeta\zeta}(3\sin^2\beta - 1)\frac{1}{2}$$

$$\delta zz_1 = \delta_{\zeta\zeta cyl} \; S \text{ and } \delta zz_2 = -1/2 \; \delta_{\zeta\zeta} \; S$$

Here we presumed a fast hindered rotation of the molecules around their long axes, which generates an axial symmetric shift tensor. In the case of a fast dynamic of the molecules around the column axis only one line with an averaged shift is seen

$$\delta zzm = 1/2(\delta_{\zeta\zeta cyl} - 1/2 \; \delta_{\zeta\zeta})S.$$
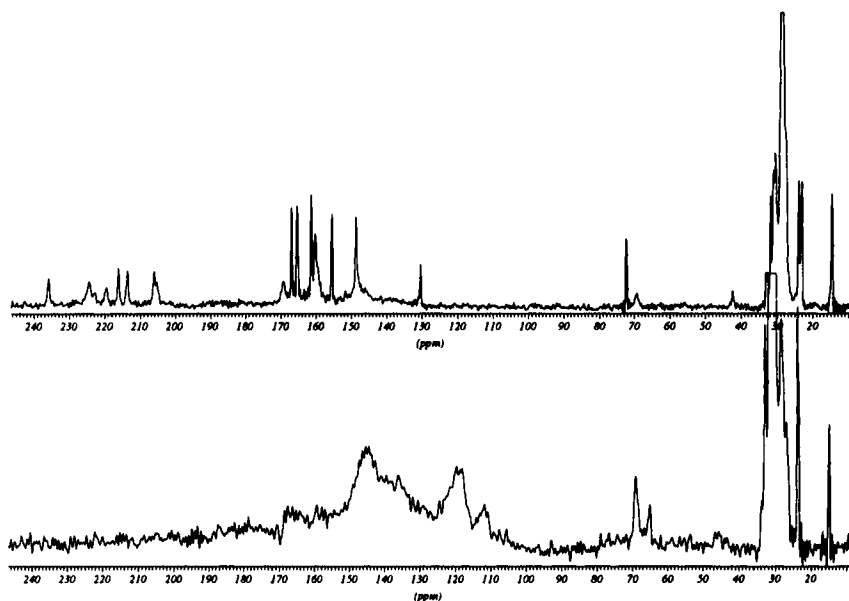
FIGURE 8 The spectra in the smectic (above) and T phase (below) demonstrate the drastic change at the transition. The resolution is reduced, but the behavior concerns all lines in a similar way. The typical new line shape is best visible for -OCH2 (x1) at 72 ppm

For the oblique columnar phase of bi-forked molecules we observed one sharp line with small anisotropy, which is typical for this fast dynamic condition.

The two phases of the swallow tailed molecules behave quite different. On the base of the model of columns we have here the situation of a slow dynamic with two singularities, best visible for x1 at around 72 ppm in Figure 8. The aromatic singularities broadens proportionally to their anisotropy. The singularity δzz_2 for the perpendicular orientations somewhat deviate from the static theoretical values, whereas the singularity δzz_1 from the parallel oriented molecules is markedly lower. We explain this reduction by a tilt of the long axis against the preferred axis. There must be a strong correlation between the perpendicular and parallel orientations since otherwise all long axes would be parallel to the strong external field. To obtain quantitative values we fitted the broad ^{13}C bands of the aromatic ortho-carbons to our model (see Figure 9). The deviation of the singularity δzz_1 delivers an angle β in the order 55°, if we assume that the order parameter S is the same as in the SmC phase. The difference in the perpendicular shift can be explained in connection with the large line width by a small contribution of translational diffusion. The reduction in the anisotropy and broadness

of the singularities points to dynamic effects with correlation times in the order of 10^{-5} s. The different intensity of the two singularities suggests a change in the radial distribution due to the strong field.
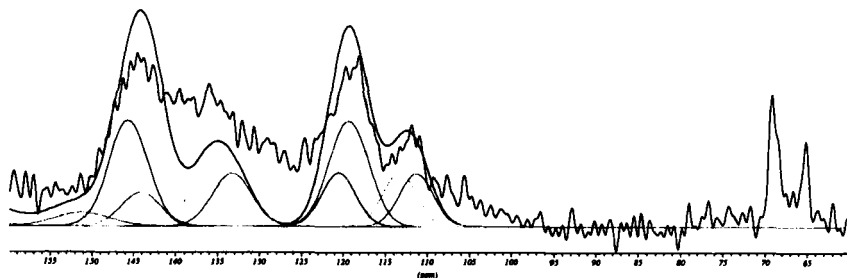
FIGURE 9 The best fit of the lines from the ortho-positions (C2, C3, C6, C7, C10, C11) to the cylindrical singularities in the T phase assuming $S_T = S_{Sc}$ and a tilt angle of 55°. The intensity in the central region contains contributions from other azimuth angles and other positions

MOLECULAR CONFORMATION AND PACKING IN THE OBSERVED STRUCTURES

The NMR investigations lead to a molecular model in which the aliphatic tails are inclined with respect to the aromatic core. Starting from the assumption that the difference of the cross-sections between the aromatic core ($\sigma_{ar} = 0.22$ nm^2) and the aliphatic chains ($2 \times \sigma_{al} = 0.36$ nm^2) can be equalized by a tilt of the core, a tilt-angle between both can be estimated by $\beta = \cos^{-1} 0.22/0.36 = 52°$. Such a configuration has been proved by single crystal structure analysis of bi-forked compounds, too[35].

Smectic C phase

Comparing the d-values within the homologues of the series **A** no significant dependence on the chain lengths can be observed. Therefore it is assumed that the aliphatic chains are more or less disordered but – one average – aligned parallel to the layer normal (see Figure 11). They give rise to the closed outer diffuse scattering (see Figure 4b). If the increase of the d-values by the insertion of an additional benzene ring $\Delta = d(B6-12)-d(A5-12) \cong 0.3$ nm is compared with the length of the inserted segment ($\cong 0.6$ nm) an angle of 60° can be estimated. Therefore the aromatic core should be tilted by a similar angle. That is proved by the pattern of a monodomain in the SmC phase (see Figure 2b).
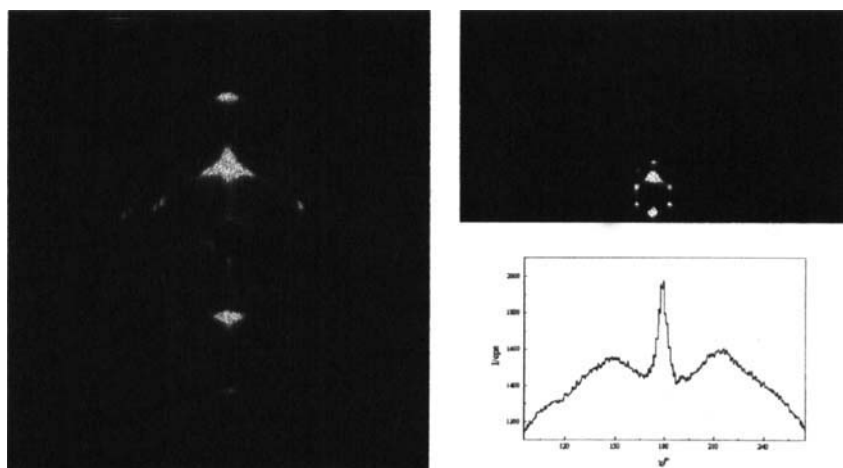
FIGURE 10 Patterns in the Col_{rect} phase of compound **B6–12** on the left side: small angle region, on the right side: diagram together with a scan along the outer diffuse scattering (χ-scan) (See Color Plate V at the back of this issue)

TABLE V Layer thickness and tilt angle in the SmC phases

Compound	d_{exp} in nm	β_{exp} in °
A5–10	3.74	not measured
A5–11	3.90	not measured
A5–12	3.92	not measured
A5–13	3.94	50.0
A5–14	4.08	49.0
B6–12	4.20	56.0
B6–13	4.24	54.5

The above mentioned diffuse maximum on the outer diffuse scattering which indicates a tilt of about $\beta_{exp} \cong 55°$ is caused by the aromatic core. The tilt angles β_{exp} in the SmC phase of the investigated compounds are listed in Table V.

Columnar phase

The pattern of an oriented sample (see Figure 10) now exhibits two outer diffuse scattering maxima positioned symmetrically to the meridian and additional reflections in the small angle region. The pattern points to a two-dimensional rectangular centred cell. Only reflections with Miller indices h+k = 2n can be

SmC   Col$_{rect}$
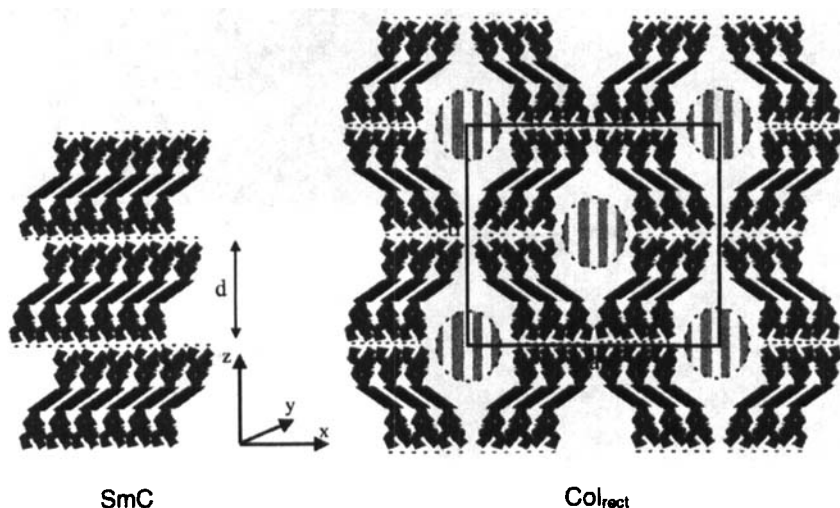
FIGURE 11 Structural model of the SmC and Col$_{rect}$ phase

observed. The Table VI summarizes the experimental values. But the pattern also demands a doubling of the translation period in comparison with the d-value of the SmC phase. The modelling of such a structure is not evident. But the pattern clearly proves that the cores are tilted symmetrically to the normal. (which is now the b-axis). Although it cannot be excluded that this symmetrical alignment is a result of a macroscopic rotational disorder of the sample, the formation of the structure by cooling a monodomain led us to the model with alternating tilt directions in neighboured building groups. (see Figure 11). Because of the high tilt angles of the aromatic cores this packing contains defects which are indicated in the figure 11 by hatched zones (regions of reduced density). These defects build the two-dimensional lattice. The structure contains glide planes parallel to the a and b vector at a/4 and b/4 as well as mirror planes parallel to the a and b vectors at a/2 and b/2. This is the symmetry of the two dimensional space group c2mm (No 9)[36].

The structure of the columns perpendicular to the layer have been commonly explained by a stack of the branched molecules the long axes of which are perpendicular to the column axis and rotationally disordered around this axis[25,26]. In this way the aliphatic tails form an envelope around the aromatic core and the concept of the segregation between hydrophilic and hydrophobic parts can be applied[28]. But, such a formation of the columns can be definitely excluded in the phases under discussion since the existence of the outer diffuse scattering

maxima allow only two tilt directions (or a tilt along a cone). Therefore we have to assume that the molecules in the next planes (above and below the drawing plane) have the same orientation. It can be the reason for the appearance of the three-dimensional phase, since the driving forces for breaking the smectic layer in x direction should be similar to those in y direction (the z axis is parallel to the layer normal). The small existence range of the columnar phase and their strong dependence on the experimental conditions support this assumption.

TABLE VI Observed and calculated Bragg angles and lattice parameters in the Col_{rect} phase of compound **B6–12** and **B6–13**

Compound	B6–12		B6–13	
(hk)	θ_{exp} *in* °	θ_{ber} *in* °	θ_{exp} *in* °	θ_{ber} *in* °
0 2	1.10	1.10	1.07	1.06
1 1	1.20	–	1.25	–
1 3	1.98	1.97	1.99	1.96
0 4	2.20	–	2.11	–
lattice	a = 4.10 nm		a = 3.89 nm	
parameter	b = 8.02 nm		b = 8.36 nm	

Tetragonal phase

Caused by the screw axis (4_1 axis) the calculated lattice parameter c corresponds to four times the d-value of the SmC phase. It can be achieved, if in the packing of the columnar phase the molecules of each second and third layer are turned out of the drawing plane. Since only one extinction rule could be observed (001: l = 4n) the space groups No.76, No.78, No.91, No.92, No.95 and No. 96 (according to[36]) must be considered. A distinction between them cannot be given at the present state of the work. The calculated lattice parameter are listed in Table VII.

The Figure 12 shows a possible packing of the molecules in the lattice, which contains the 4-fold screw axes. The packing is derived from that of the columnar structure in the way, that the molecules of each second and fourth layer are tilted out of the drawing plane (up and down). With respect to the defects as the base for the structure the interpretation resembles that of the SmQ phase, which is proved to be a three-dimensional TGB phase[39]. Also there lattices with tetragonal or hexagonal symmetries are formed based on defects which are caused by twisted grain boundaries. The existence of the twisted grain boundaries are connected with a break of symmetry e.g. by chiral compounds. This can be excluded for the compounds under discussion. But the frustration between different

S. DIELE *et al.*

cross-sections of different moieties within the molecules in connection with an average tilt of the molecules results, too, in a break of the smectic layer and in a constitution of a three-dimensional periodicity.

TABLE VII Lattice Parameters of the T Phase

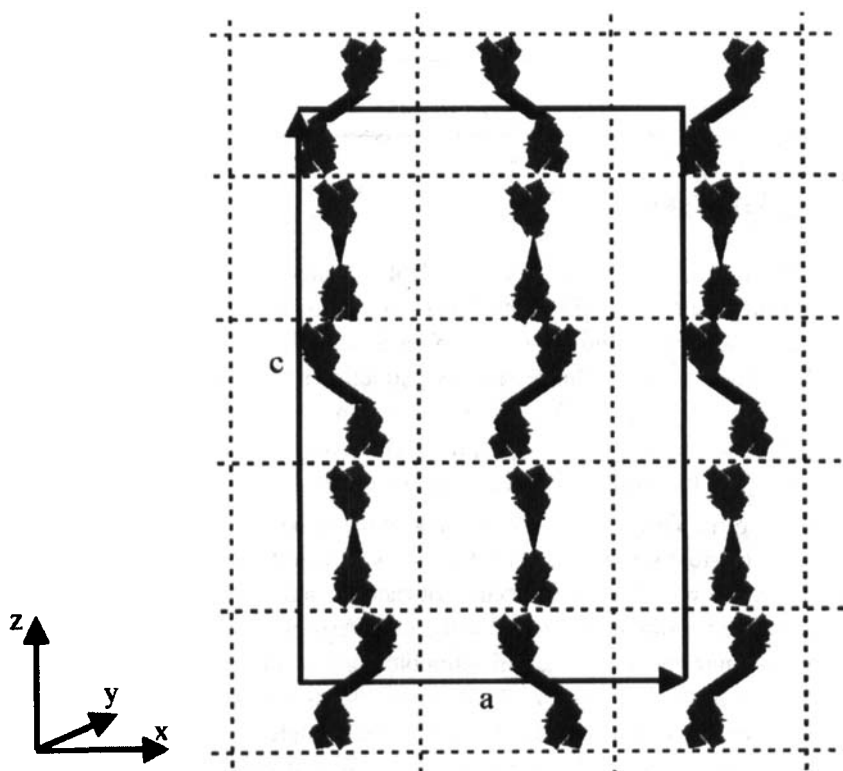| Compound	Lattice Parameter	
	a in nm	*c in nm*
A5–13	11.07	15.69
A5–14	11.00	15.55
A5–16	10.59	15.41
B6–13	11.10	16.12
B6–16	11.39	17.14

FIGURE 12 Sketch of the packing in the tetragonal phase. In the second and fourth layers the molecules are assumed to be turned out of the drawing plane

CONCLUSIONS

By X-ray diffraction measurements on monodomains the structure of the SmC-, Col- and tetragonal (T) phase of double-swallow tailed compounds is discussed. The transition between these phases is mainly explained by a different packing of the aromatic middle part of the molecules whereas the aliphatic chains adopt a more or less disordered state.

In a monodomain of the SmC phase the middle parts are inclined by an angle of about 50° with respect to a preferred direction (layer normal). With decreasing temperature a tilt in two directions (+/-50°) can occur which leads to a break of the layer. The break causes a density modulations within the layers, so that a two-dimensional rectangular structure is formed. In the low temperature phase the existence of a four-fold axis is proved on an X-ray pattern, which was evaluated on the base of a three-dimensional (tetragonal) lattice. It can be explained by a model where in addition to the two-dimensional phase the middle parts of the molecules of each second layer are turned out of the drawing plane and forms a screw axis parallel to the c axis.

With respect to the packing the structures of the liquid-crystalline phases under investigation seems to be different to those of the bi-forked compounds. In the later ones the structures are built up by rods, in which the middle parts of the molecules are aligned perpendicular to the cylinder axis but randomly in direction of the cylinder axis. In this connection it should be emphasised that the Col and T phases under investigation appear always as low temperature forms in contradiction to those of the bi-forked compounds.

References

[1] G. Sigaud, F. Hardouin, M.F. Achard and A.M. Levelut, J. Phys. (Paris), **42**, 107 (1981).
[2] F. Hardouin, A.M. Levelut, M. Achard and G. Sigaud, J. Chem. Phys., **80**, 83 (1983).
[3] P.G. deGennes and J. Prost, The Physics of Liquid Crystals, Oxford Science Publications 1993.
[4] B.I. Ostrovski, Liq. Cryst., **14**, 131 (1993).
[5] J.F. Rabolt, T.P. Russell and R.J. Twieg, Macromolecules, **17**, 2786 (1984).
[6] W. Mahler, D. Guillon and A. Skoulios, Mol. Cryst. Liq. Cryst. Lett., **2**, 111 (1985).
[7] H.T. Nguyen, G. Sigaud, M.F. Achard, F. Hardouin, R.J. Twieg and K. Betterton, Liq. Cryst. **10**, 389 (1991).
[8] J. Höpken and M. Möller, Macromolecules, **25**, 2485 (1992).
[9] T.A. Lobko, B.I. Ostrovski, A.I. Pavluschenko and S.N. Sulianov. Liq. Cryst. **3**, 361 (1993).
[10] S. Diele, D. Lose, H. Kruth, G. Pelzl, F. Guittard and A. Cambon, Liqu. Cryst., **5**, 603 (1996).
[11] M. Ibn-Elhaj, A. Skoulios, D. Guillon, J. Newton Hodge, and H.J. Coles, J. Phys. II France, **6**, 271 (1996).
[12] S. Pensec and F. Tournilhac, Chem. Commun., 441 (1997).
[13] W. Luzzati, H. Mustacchi and A. Skoulios, Nature, **180**, 600 (1957).
[14] A. Skoulios and W. Luzzati, Acta Cryst., **14**, 278 (1961).
[15] C.E. Fairhurst, St. Fuller, J. Gray, M.C. Holmes and G.J.T. Tiddy in Handbook of Liquid Crystals Vol. III, ChapterVII, ed. by D. Demus, J. Goodby, G.W. Gray, H.-W. Spiess and V. Vill, Wiley. VCH 1998.
[16] C. Tschierske, J. Mat. Chem., **8**, 1485 (1998).

[17] C. Paleos and D. Tsiourvas, Angew. Chem., **107**, 1839 (1995).
[18] J. Malthete, A.M. Levelut and N.T. Nguyen, J. Phys. Lett. (Paris), **46**, L875 (1985).
[19] J. Malthete, H.T. Nguyen and C. Destrade, Liq. Cryst., **13**, 171 (1993).
[20] H.T. Nguyen, C. Destrade and J. Malthete, Adv. Mat., **9**, 375 (1997).
[21] H.T. Nguyen, C. Destrade, A.M. Levelut and J. Malthete, J. Phys. (Paris), **47**, 553 (1986).
[22] C. Destrade, H.T. Nguyen, A. Roubineau and A.M. Levelut, Mol. Cryst. Liq. Cryst., **159**, 163 (1988).
[23] C. Destrade, H.T. Nguyen, K.C. Alstermark, G. Lindsten, M. Nilsson and B. Otterholm, Mol. Cryst. Liq. Cryst., **180B**, 265 (1990).
[24] H.T. Nguyen, C. Destrade and J. Malthete, Liq. Cryst., **8**, 797 (1990).
[25] A.M. Levelut, J. Malthete, C. Destrade and H.T. Nguyen, Liq. Cryst., **2**, 877 (1987).
[26] D. Guillon, A. Skoulious and J. Malthete, Europhys. Lett., **3**, 67 (1987).
[27] B. Gallot, A. Skoulios, Kolloids Z., **213**, 143 (1968).
[28] Y. Fang, A.M. Levelut and C. Destrade, Liq. Cryst., **7**, 265 (1990).
[29] W. Weissflog, A. Wiegeleben, S. Diele, D. Demus, Cryst. Res. Technol., **19**, 983 (1984).
[30] S. Diele, K. Ziebarth, G. Pelzl, D. Demus, W. Weissflog, Liq. Cryst., **8**, 211 (1990).
[31] W. Weissflog, M. Rogunova, I. Letko, S. Diele and G. Pelzl, Liq. Cryst., **19**, 549 (1995).
[32] W. Weissflog, M. Rogunova, I. Letko, S. Diele and G. Pelzl, Liq. Cryst., **21**, 13 (1996).
[33] W. Weissflog, I. Letko, S. Diele and G. Pelzl, Adv. Mat., **8**, 76 (1996).
[34] W. Weissflog, A. Saupe, I. Letko, S. Diele and G. Pelzl, Liq. Cryst., **20**, 483 (1996).
[35] J.B. Bideau, G. Bravic, M. Cortrait, H.T. Ngyuen and C. Destrade, Liq. Cryst., **10**, 379 (1991).
[36] International Tables for X-Ray Crystallography, Vol. I, ed. by N.F.M. Henry and K. Londsdale, The Kynoch Press Birmingham, 1952.
[37] U. Nütz S. Diele, G. Pelzl, H. Ringsdorf, W. Paulus and G. Wilson Liqid. Cryst. **18**, 699 (1995).
[38] D. Guillon in Liqid Crystals II ed by D.M.P. Mingos, Springer-Verlag, Berlin Heidelberg New York, 1999.
[39] A.M. Levelut, E. Halloin, D. Bennemann, G. Heppke and D. Lötzsch, J. Phys. II (France), **7**, 981 (1997).